© 2018 IJSRST | Volume 4 | Issue 5 | Print ISSN: 2395-6011 | Online ISSN: 2395-602X
Themed Section: Science and Technology

# Strength Validation of Hexagonal Cellular Spoked Non-Pneumatic Tires for Automobiles through Finite Element Analysis

**Mihir Mangesh Pewekar[1],Sambhaji D. Gaikwad[2]**

[1]Department of Mechanical Engineering, Rajiv Gandhi Institute of Technology, Mumbai, Maharashtra, India

[2] Assistant Professor, Department of Mechanical Engineering, Rajiv Gandhi Institute of Technology, Mumbai, Maharashtra, India

## ABSTRACT

Composite materials and structures can be said to be major paradigm of the current scientific revolution. Large scale adoption of such a paradigm has led to the invention of Non-Pneumatic tires also called as "Airless Tires". In this paper, attempt to study the deformation mechanisms of the honeycomb cellular structure is made. A lower contact pressure is obtained with the NPTs than with the pneumatic tire due to the decreasing spoke stiffness of the NPTs when they are designed to have the same load carrying capability. The deformation mechanisms are validated through the Finite element prediction on ANSYS Mechanical APDL solver. This document focuses on the adaptation for of NPT's for automobile only. The study of this adaptation is conducted through the consideration of four cases of loading: Compressive, lateral Shear, Lateral Torsion, Circumferential torsion. A tire cannot be inducted into service without validation of strength in these types of loadings. This document on restrict the analysis to independent analysis of each loading in the FEA environment. These afore-mentioned loadings are discussed and quantified for strength validation of these type of tires. The primary investigation consists of the localised stress concentration, maximum deflection and deformation shapes in the cellular spokes and the contact stresses at the tire road interface. This document consists of two set of results the quantitative and the qualitative. The conclusions are drawn on the foundation formed by these sets of results.

**Keywords**: Airless Tire, hexagonal cellular structure, honeycomb, automobile, composites.

## I. INTRODUCTION

The road transport industry has been dominated by pneumatic tires for more than 100 years. The introduction of pneumatic tires was a major paradigm in the transport industry and is still used with certain development to improve performance. Many research individuals and giants in the field of tire technology have introduced compliant spokes to replace air of the pneumatic tire. Pneumatic tires have the following advantage [3]-

- low energy loss on rough surfaces
- low vertical stiffness
- low contact pressure compared to solid wheel
- low mass as compared to **solid wheel**.

But, pneumatic tires also have the following disadvantages [3]:

- the possibility of catastrophic damage – a flat while driving
- the required maintenance for proper internal air pressure
- the complicated manufacturing procedure

Mishaps due to these can be quite fatal in consideration of human safety.

Finite element results standalone cannot create the understanding of the nature and behaviour of the material. It requires certain degree of analytical background and theory which can help in understanding the predictions made by the finite element solver. The approach of involving analytical methodology and numerical analysis gives a certain amount of strength to the advancement in the technology. Thus, the paper will represent such a methodology which intends to advance the study in this unique piece of scientific revolution.

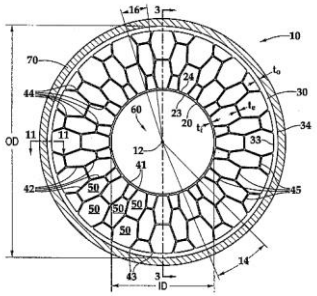

**Figure 1.** Original NPT patented in year 2007(US20120234445 A1)

Lorna Gibson [2] has given many insights to the analysis of in-plane loading of honeycomb structures. This theory can be extensively used and the relation for the NPT can be explicitly derived. Sassi et. al. [8] has given the methodology and the materials required for the FEA solver to predict the deformation shapes with adequate accuracy or convergence. Jaehyung Ju et.al. [5] have given in-depth methodology of analysis of the flexible cellular spokes. They have considered different geometries for the flexible spokes under the same loading and analysis is conducted. Jaehyung Ju et.al. [4] have given the comparison of static contact pressures of NPT with standard pneumatic tires. The literature, at the present stage, has indicated the static validation of the structure under only one type loading condition subjected to an automobile tire. But the behavior of the tire under different loading conditions is yet to be explored. This document only considers static loading in each case (Dynamic conditions not considered).

This document is structured to make profound inferences based on the stress stain analysis, thus the section II discusses the methodology with which the analysis is conducted. Section III will ponder upon the geometry and the relations that lead to the dimensions of the Tire in physical domain. It will also contain the CAD modelling of the tire which will form the physical domain for the Finite Element Analysis. Section IV will consist the various inferences and graphical representations obtained from the software.

## II. METHODOLOGY

An effort to incorporate this type of a mechanical structure in automotive transport, it is necessary to analyse its behaviour under different types of loading. A tire of an automobile is subjected to the following types of loading:

Case 1: Translation by application of torque (Pure rolling of the wheel)-**Circumferential torsion**
Case 2: Compressive forces due to the weight of the vehicle- **Buckling and shear of individual spokes**.
Case 3: Cornering (during Turning)- **Lateral Shear**
Case 4: Manoeuvring (Steering of the front/rear wheels)-**Lateral torsion**

Quantification of the loading:
To conduct an effective finite elemental analysis, it is essential to quantify the forces in each loading type. The quantification is performed as follows.

### Case 1: Circumferential Torsion

The circumferential torsion is heavily based on the vehicle to be considered. In this document we have considered a complaint tyre for 245/65R19 pneumatic tire. A general survey was made for the major SUV's, in the market, that are in the use of this tyre. The

mean of the engine torque rating was considered for the analysis. This analysis is essential as the starting torque is higher than the torque required to keep the vehicle in motion. The summary of the survey is provided in tabular form in Table 1. The torque rating considered is 225 Nm

**Table 1.** Data pertaining to the torque rating of Sports utility vehicles (source: https://www.auto123.com/)

| Vehicle (Model and year) | Mazda Tribute 2004 | Ford ranger XLT 2009 | Toyota highlander 2009 | Nissan X-trail XE 2005 |
|---|---|---|---|---|
| Torque (Nm) | 242 | 220 | 280 | 195 |

**Case 2: Compressive Loading**

The compressive loading on each tire is dependent of the weight of the vehicle and the distribution of weight between the front and rear axle. In this case, we have considered the vehicles considered in case 1.

**Table 2.** Data pertaining to the weight of Sports utility vehicles (source: https://www.auto123.com/)

| Vehicle (Model and year) | Mazda Tribute 2004 | Ford ranger 2005 | Toyota highlander 2009 | Nissan X-trail XE 2005 |
|---|---|---|---|---|
| Weight (Kg) | 1612 | 1442 | 1895 | 1416 |

From the general survey available in the table 2 we can consider the average weight (including weight of the passengers) as 1800 kg. Assumption is equal distribution of weight on the four tires.

$$N = \frac{W}{4} = 450\ kg = 4500\ N \qquad 1.$$

**Case 3: Cornering (Lateral Shear)**

During the turning of the vehicle along a curved path, the tendency of the vehicle to move outward due to the action of centrifugal force is countered by the friction between the road and the tyre. This condition generates a laterally opposing forces on the tyre which are separated by certain distance. This force experienced by the tyre is called as the cornering force. The force generated lateral shear stresses in the cellular spokes.

The cornering force is the function of the slip ratio and the velocity of the vehicle. These forces during the turning of the vehicle are shown in Figure

According to Moustapha Doumiat et.al. (2010) [8], the cornering force is expressed by the following relation.

$$F_{yij} = -C_{\alpha i}.\tan(\alpha_{ij}).f(\lambda) \qquad 2.$$

$$f(\lambda) = (2-\lambda)\lambda \quad if\ \lambda < 1 \qquad 3.$$
$$f(\lambda) = 1 \quad if\ \lambda \geq 1$$

Where,

$\lambda = \frac{\mu F_{zij}}{2C_{\alpha i}|\tan(\alpha_{ij})|}$

$F_{yij}$ is the lateral force (cornering force) on the tire.

$F_{zij}$ is the normal load on the tire.

$\alpha_{ij}$ is the slip angle.

$C_{\alpha i}$ is the lateral stiffness of the tire.

Moustapha Doumiat et.al. (2010) [8] have also estimated that the vehicle maintains stability when the centripetal acceleration is less than 0.4 times the gravitation acceleration constant. Thus, for validation, the use of this constitutive relation is justified.

Thus, for a limiting case,

$$F_c = (0.4 \times g)\frac{P}{g} = 1.4\ KN \qquad 4.$$

Where,

g is the gravitation acceleration constant (9.81 $ms^{-1}$)

N is the Normal force on each tire (P) (average of the weight in Table 2.). (P = 350 kg)

### Case 4: Lateral Torsion

The lateral torsion occurs during the rotation of the wheels about the z axis shown in Figure. This action is performed by the steering mechanism in the car. This resistance to the motion of the tire is quite complex to quantify. But the mechanism can be studied. Whenever static loading is considered, the contact between the tire and the road forms a patch of contact. The lateral torsional stiffness as given by friction in pneumatic tire by [3]. The empirical relations of tire frictions and steering torque are available but cannot be applied to non-pneumatic tires without verification of its applicability. thus, using an approximate method of determination of resisting torque.

**Assumptions made for the quantification are:**

1. The pressure varies uniformly at the patch of contact as shown in Figure. This assumption is made based on contact pressure result obtained in the FE analysis shown in Figure.
2. The shear band in the tire is manufactured compliant with the TW 300(treadwear factor in pneumatic tires).
3. The coefficient of friction is 0.91. (using the previous assumption and the relation from [7], $\mu = \frac{2.25}{TW^{0.15}}$)
4. The resistance to the motion of rotation about the z-axis is resisted only by the frictional force the line where pressure is maximum.
5. Due to absence of the inflation effect of the tire, the lateral width of the contact area is equal to the width of the tire.

As per Figure.10 the red region shows the area which has highest pressure of 0.33 MPa, Figure. 2 shows the distribution as per first assumption.

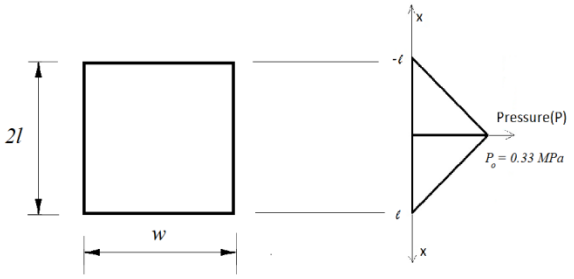


**Figure 2.** Pressure distribution over the contact area

The reaction force is distributed over the area of the patch. Thus, the using the force pressure relationship over an elemental area. Taking the elemental strip of width equal to the lateral width of the patch.

$$N = \int dN = \int P(x)dA \quad (5.)$$

$$dA = dx \times w \quad (6.)$$

$$\therefore N = \int_{-l}^{l} P(x)dx.w \quad (7.)$$

$$N = 2\int_{0}^{l} P(x)dx.w$$

Where,

N is the reaction force from the ground.

$P_o$ is the maximum pressure over the area.

$l$ is the semi-length of the contact area.

$w$ is the width of the tire (according to fifth assumption equal to width of contact area).

In previous case we have calculated the loading on the tire, thus

$$normal\ reaction = 4906\ N$$

Integrating Eq (7),

$$N = wlP_o \quad (8.)$$

$$l = \frac{4906}{0.33\times10^6\times0.245} = 0.055 \text{ mm} \quad (9.)$$

As per the fourth assumption, the resisting torque is provided by the uniformly distributed load at this line. Thus, the limiting value of this torque,

$$Frictional\ force(F) = \mu\ N$$

$$T = \int_{0}^{\frac{w}{2}} F\ .dr = F.\frac{w}{2} = \frac{\mu N w}{2} \quad (10.)$$

$$T = 546\ Nm$$

## III. PREPARATION OF THE CAD MODEL

The CAD model is prepared in the SOLIDWORKS software. The primary task in this step is determination of dimension of the cellular spokes.

**Determination of appropriate wall thickness and the edge length of the hexagonal cells:**

The basic analysis of this structure is based on the works of Lorna J Gibson [2]. The analysis uses the basic study of deformation mechanisms in uniaxial and biaxial in-plane loading published in her study. This unique approach is aimed to replace pneumatic tires, thus is considered to have the stiffness properties of the tire to be equal. The following formulae from the afore mentioned book are used-

$$\frac{E_1^*}{E_s} = \frac{E_2^*}{E_s} = (\frac{t}{l})^3 \times \frac{\cos\theta}{(h/l + \sin\theta)\sin^2\theta} \quad 11.$$

$$\frac{G_{12}^*}{E_s} = (\frac{t}{l})^3 \times \frac{h/l + \sin\theta}{\left(h/l\right)^2\left(1 + \left(2h/l\right)\right) COS\,\theta} \quad 12.$$

The above equation contains the two unknown variables i.e. the thickness of the spokes and the resultant modulus of the structure. Thus, the solution requires Nonlinear optimization techniques (Numerical techniques are provided by MATLAB software). Another approach: Selecting an arbitrary tire (say 245/70 R17.). Based on the standard Notation finding the essential parameters for geometric modelling. Now, keeping these values relevant we fix the edge length with certain necessary approximations (method adopted may not be suffice for design, but acceptable for computational validation).

For regular hexagon (h = l, θ = 30º) the above formula reduces to,

$$\frac{E_1^*}{E_s} = \frac{E_2^*}{E_s} = 2.3(\frac{t}{l})^3 \quad 13.$$

$$\frac{G_{12}^*}{E_s} = 0.57\,(\frac{t}{l})^3 \quad 14.$$

Based on the literature review the wall thickness is taken as 5 mm. As larger thickness would result in lower stress concentration.

Edge length calculation:

Aspect ratio = 70 %

Width of tire(s) $= 245 \times 0.70 = 172$ mm

As shown in Figure 3.,the edge length is found out using the width of tire.

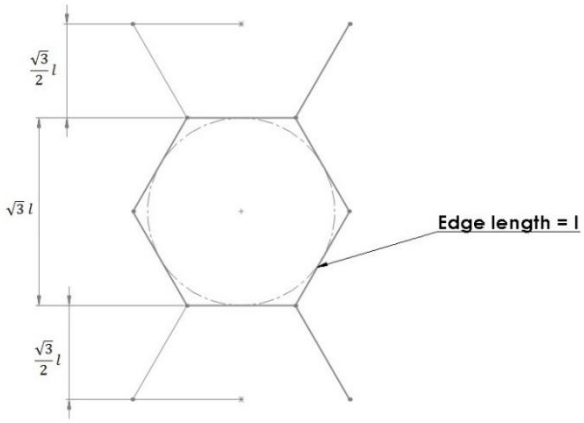


**Figure 3.** shows the geometrical derivation of the width of the side wall

$$Total\ height = 2\sqrt{3}\,l \quad 15.$$

The above Eq (9) is equated to the side wall thickness to obtain a compliant tire for the vehicle.

Therefore,

$$2\sqrt{3}\,l = s = 172$$

$$l = 46\ mm$$

Using the Eq (7)

$$\frac{E_1^*}{E_s} = \frac{E_2^*}{E_s} = 2.3(\frac{3}{46})^3$$

$$\therefore E_1^* = E_2^* = 0.020\ \text{MPa}$$

Using the Eq (7)

$$\frac{G_{12}^*}{E_s} = 0.57\,(\frac{t}{l})^3$$

$$G_{12}^* = 5.06 \times 10^{-3} MPa$$

The equivalent moduli obtained are small hence would result in lower contact pressures. The actual stiffness will be comparatively higher due to the use of inner and outer metallic rings (discussed in section IV). This method can be accepted to be quite inadequate in the design such an integral component of an

automobile, where safety is a prime concern. But this approach is well justified considering our aim to initially validate before getting into its use as commercial alternative to traditional tires. Based on the above derived nominal thickness and edge-length, generating a CAD model used for further computation techniques.

### CAD- Model

The CAD model is generated in the industrial design software -SOLIDWORKS. The CSG approach is used in this design.

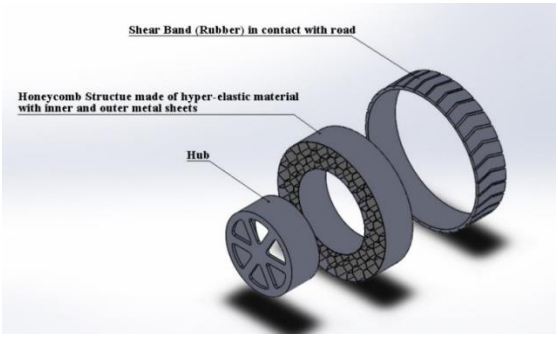


**Figure 4.** The CAD Generated model of the Tyre explaining the division of the structure.

## IV. MATERIAL OF THE CELLULAR STRUCTURE

Figure. 4 shows an NPT made up of the honeycomb spokes and tread components. The inner face-sheet is made of an aluminium alloy (7075-T6; density, q = 2800 kg/m3, Modulus, E = 72 GPa, and Poisson's ratio, m = 0.33) and functions as a rigid hub. A 1 mm thick aluminium alloy is used for the inner face sheet (hub). The outer face-sheet, made of a high strength steel (ANSI 4340; density q = 7800 kg/m3, E = 210 GPa, and m = 0.29), is set to be 0.5 mm. This enforces the tread rubber to be deformed by shear. Without the outer face-sheet, the edges of the spokes over the contact zone with the ground would buckle and cause an undesirable nonlinear effect of the honeycombs. Polyurethane (q = 1200 kg/m3, E = 32 MPa, shear modulus, G = 10.81 MPa, and m = 0.49) is used as the constituent material of the honeycomb spokes (core) and its uniaxial, bi-axial, and planar tension test results are available in ANSYS material data module. The three test results are used as a hyper elastic material input of the polyurethane honeycomb spokes in the ANSYS. The honeycomb spokes have a 5-mm wall thickness. The tread component is made of a rubber (q = 1043 kg/m3, E = 11.9 MPa, G =4 MPa, and m =0.49). It is also used for the hyperplastic model in the ANSYS Mechanical APDL. The thickness of the tread is Figure. 3 shows an NPT made up of the honeycomb spokes and tread components. The analysis of the honeycomb cellular spokes is performed using the Ogden model for hyper elastic materials. The Ogden model is used based on the validation statements put forth by Z. Nowak [13].

## V. FINITE ELEMENT ANALYSIS

The CAD model in used as the physical domain for the FE analysis, the details of the CAD model are in section III. The material properties for the FE analysis are discussed in section IV. Now we conduct the analysis as per our methodology discussed in section II. The quantification of the forces is mentioned in section II. The FE analysis is conducted in Mechanical APDL using the ANSYS workbench interface. For validation, the analysis is performed statically i.e. the forces are constant and do not vary in direction or in magnitude with time. The analysis is also divided as per the cases mentioned in section II.

### Quantitative results: Finite Element Analysis Contour Plots

### Case I: Circumferential Torsion

Average loading of the 225 Nm is applied based on the survey discussed in section II. The results obtained are summarised in Table 3.

**Table 3.** Summary of FEM results

| Torsional Loading (Nm) | Anglar Deflection (Deg) | Maximum Von Mises stress(MPa) |
|---|---|---|
| 225 | 0.57 | 0.24 |

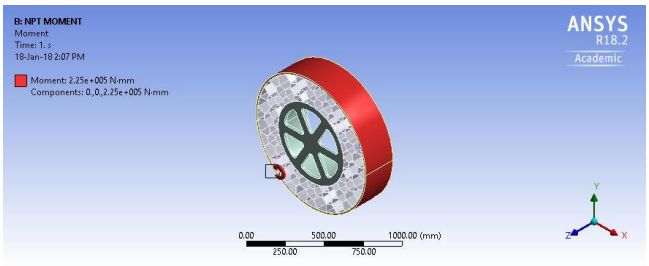


**Figure 5.** Indication of direction of loading

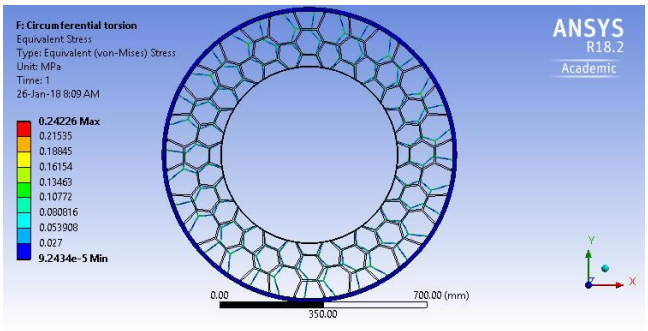


**Figure 6.** The pictorial presentation in method of contour plots of Von-misses Stress.

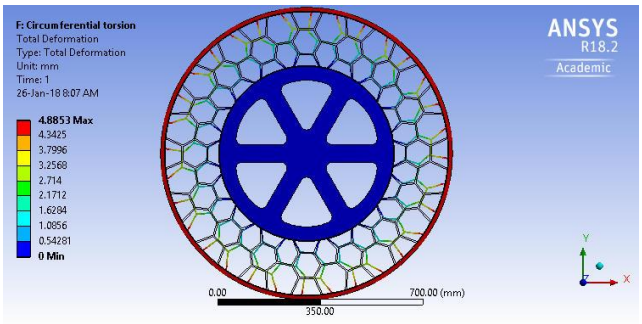


**Figure 7.** The pictorial presentation in method of contour plots of Deformation.

### Case 2: Compressive loading – Buckling and shear of individual spokes

Average loading of the 4375 N is applied. The results obtained are summarised in Table 4.

**Table 4.** Summary of FEM results

| Load (Nm) | Deflection of HUB in Y-axis (mm) | Maximum Von Mises stress(MPa) |
|---|---|---|
| 4500 | 16.1 | 1.985 |

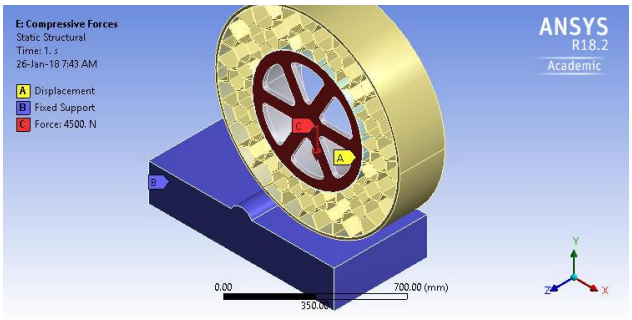


**Figure 8.** Indication of direction of loading

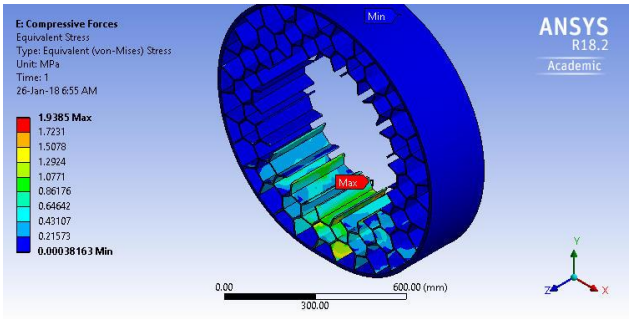


**Figure 9.** The pictorial presentation in method of contour plots of Von-misses Stress

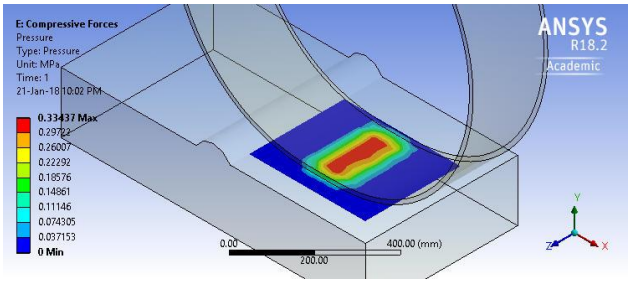


**Figure 10.** Distribution of the Contact pressure

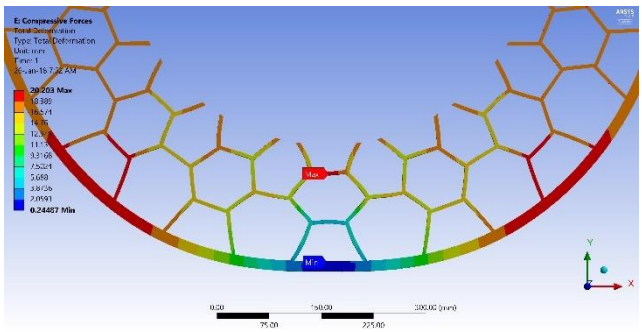


**Figure 11.** Shows the Deformation shapes

### Case 3: Cornering – Lateral Shear

Average loading of the 1400 N is applied in the Z direction. The loading in this case is combined with the compressive loading. The results obtained are summarised in Table 5

**Table 5.** Summary of FEM results

| Load in Z-axis (N) | Deflection in the Z-axis (mm) | Maximum Von Mises stress(MPa) |
|---|---|---|
| 1400 | 62.476 | 4.1882 |

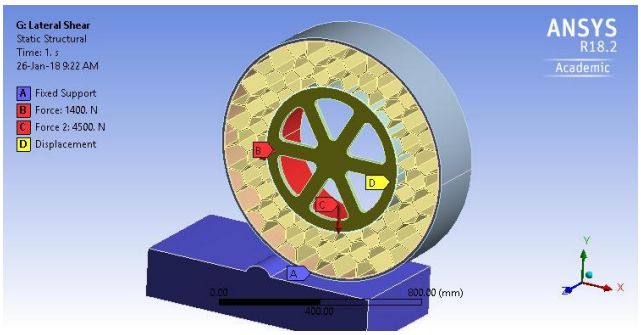


**Figure 12.** Indication of direction of loading

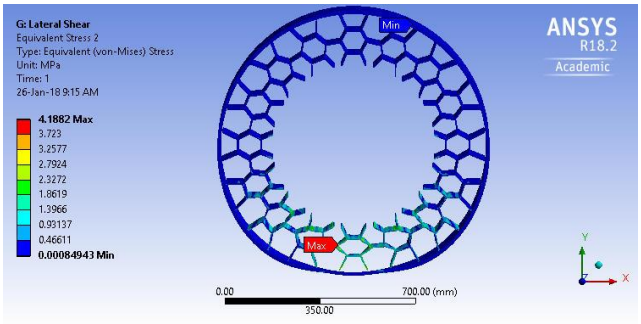


**Figure 13.** The pictorial presentation in method of contour plots of Von-misses Stress

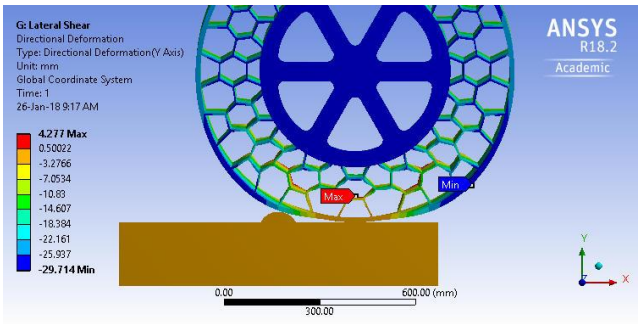


**Figure 14.** The pictorial presentation in method of contour plots of Deformation in Y-axis.

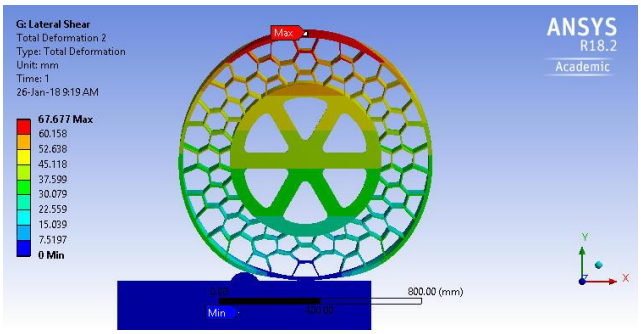


**Figure 15.** The pictorial presentation in method of contour plots of Deformation in Z-axis.

**Case 4: Steering – Lateral Torsion**

Average loading of the 5000 N is applied and rotated with 546 Nm (as calculated in section II). The results obtained are summarised in Table 6.

**Table 6.** Summary of FEM results

| Torque (Nm) | Deflection mm | Maximum Von Mises stress(MPa) |
|---|---|---|
| 546 | 6.8 | 0.67 |

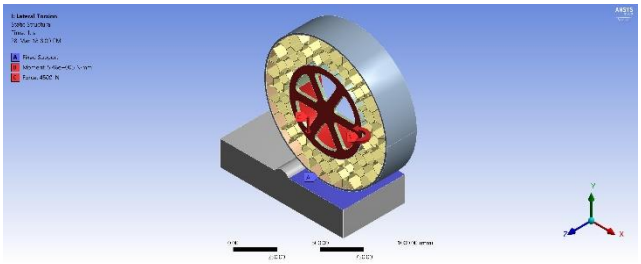

**Figure 16**. Indication of direction of loading

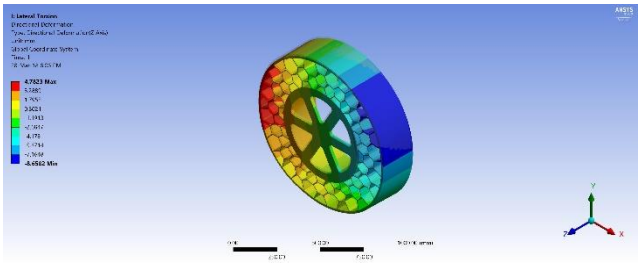

**Figure 17.** The pictorial presentation in method of contour plots of Deformation in Z-axis.

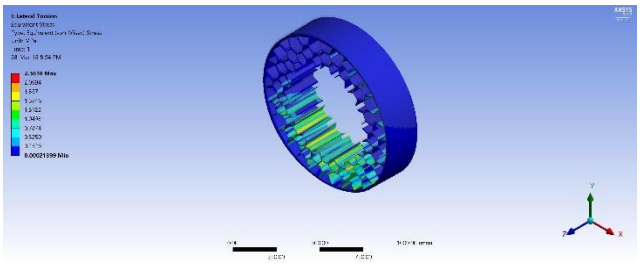

**Figure 18.** The pictorial presentation in method of contour plots of Von-misses Stress.

## Qualitative Results: Graphical Plots

The qualitative results present itself with the equivalent behaviour of the structure under the considered loading. These results give the equivalent modulus of elasticity as well as the stiffness in each loading.

### Case 1: Circumferential Torsion

Figure 17 shows the linear relationship between the stress and strain. Thus, we can say that the operation is within elastic limits.

Figure 18 show the deformations at incremental levels of the torque.

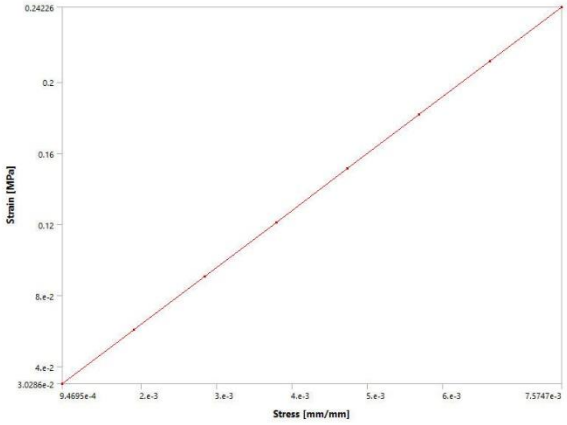


**Figure 17.** Stress-Strain Curve under torsional loading.

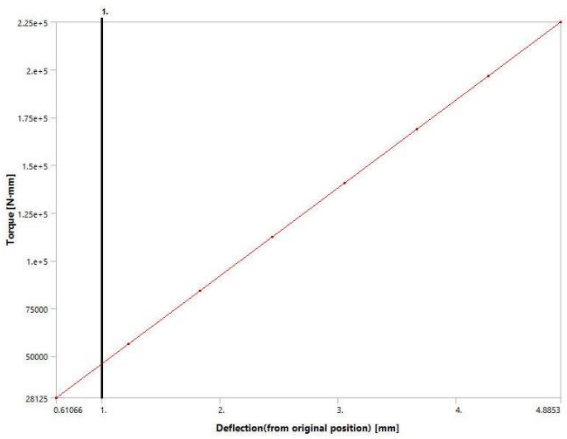


**Figure 18.** Torque vs Deflection plot.

### Case 2: Compressive loading- Buckling and shear in the spokes

Figure 19 shows the linear relationship between the stress and strain. Thus, we can say that the operation is within elastic limits.

Figure 20 show the deformations at incremental levels of the Force in the y-direction. The curve is not completely proportional to the deflection, but the variation can be neglected and assumed a straight line to find the equivalent stiffness.

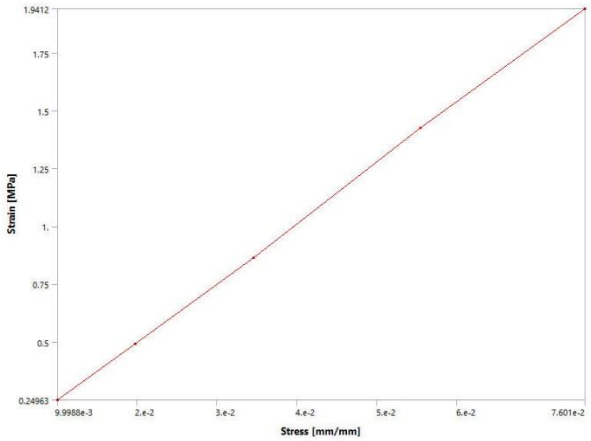


**Figure 19.** Stress-Strain Curve under compressive loading

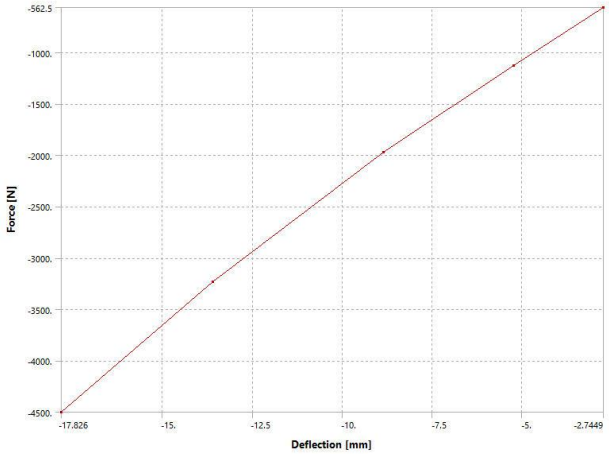


**Figure 20.** Force vs Deflection plot.

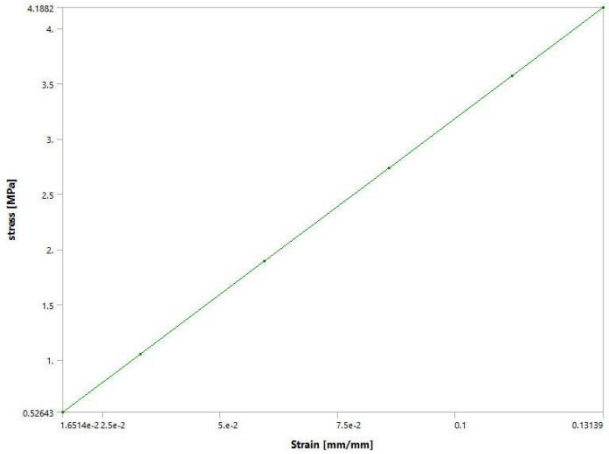


**Figure 22.** Stress-Strain Curve under torsional loading

## Case 3: Lateral Shear

Figure 22 shows the linear relationship between the stress and strain. Thus, we can say that the operation is within elastic limits.

Figure 21 show the deformations at incremental levels of the Force in the Z-direction.

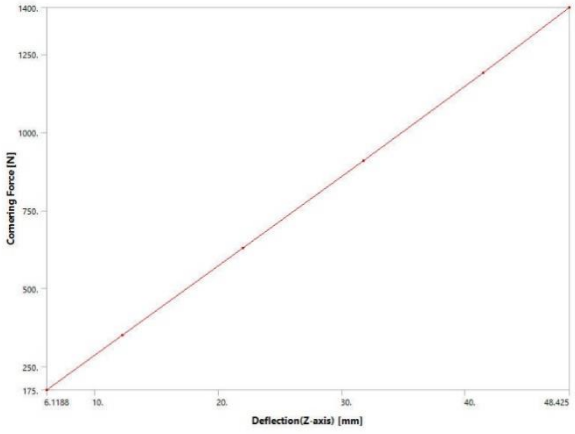


**Figure 21.** Cornering Force vs Deflection Plot.

## Case 4: Lateral Torsion

Figure 24 shows the linear relationship between the stress and strain. Thus, we can say that the operation is within elastic limits.

Figure 23 show the deformations at incremental levels of the Torque.

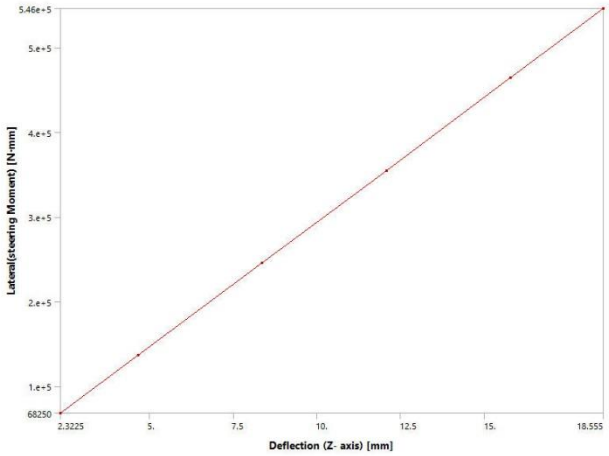


**Figure 23.** Torsion Vs Deflection Plot

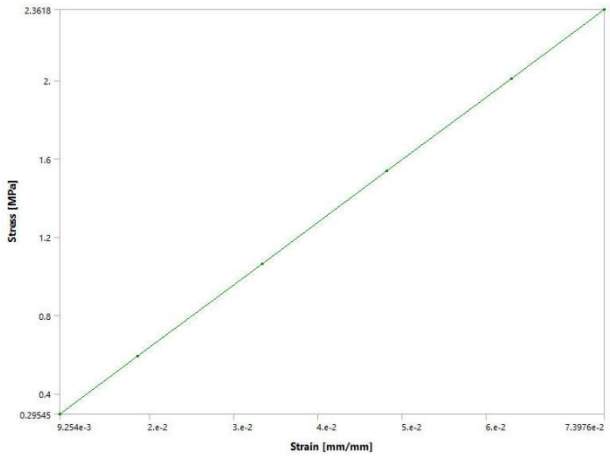


**Figure 24.** Stress-Strain Curve under torsional loading

## VI. RESULTS AND DISCUSSION

The results obtained from the analysis are incomplete without the calculation of comparable values to the pneumatic tires. The values of stiffness's are obtained from the friction in pneumatic tires [3] by Desmond Moore. The stiffness values obtained from the Qualitative plots are summarised in table 7. The torsional stiffness's are high as the hexagonal structure has different in-plane and out-of-plane properties. The out-of-plane directional equivalent modulus is higher than in-plane equivalent modulus, given by Lorna Gibson in Cellular solids [2].

**Table 8.** Comparison of Stiffness based on FEA results

| | Non-Pneumatic Tire | Pneumatic Tire |
|---|---|---|
| Torsional Stiffness (resisting torsion) | 22412 Nm/rad | 27.13 Nm/rad |
| Lateral Stiffness | 28.9 N/mm | 90 N/mm |
| Lateral torsional Stiffness | 14523 Nm/rad | 2900 Nm/rad |

The table 9 shows the behaviour of the structure through the equivalent modulus of elasticity. The equivalent modulus is low for the cellular structure, but the inclusion of the inner support rings will increase the modulus.

**Table 9.** The Modulus of elasticity from the qualitative results.

| Case | Equivalent Modulus of Elasticity (MPa) |
|---|---|
| Circumferential Torsion | 36.1 |
| Compressive loading | 25.59 |
| Lateral Shear | 32.26 |
| Lateral torsion | 31.93 |

## VII. CONCLUSION

From the Analysis in section V, we have computed by FEM, the stress developed in each type of loading an automobile is generally subjected. From the finite element results we can make the following conclusions:

- The combination of hexagonal lattice structure and hyper elastic material can be suitable for non-pneumatic tires.
- The structure is compliant for the compressive, torsional, lateral shear and the lateral torsional loading.
- The failure of this tire will occur due to the presence of the inner and outer ring due to fatigue. But by general consideration the structural integrity of the tire will not be affected as the hexagonal lattice and the shear band do not fail.
- The qualitative results show linear relationship between the results under observation, thus it can be said that the tire function under the elastic limit i.e. it is a resilient structure.
- This tire has exceptionally high torsional stiffness but low lateral stiffness. Hence, we can

conclude that additional research is to increase stiffness should be endeavoured.

## VIII. ACKNOWLEDGEMENTS

The research was supported by the Academic Research Packages provided by ANSYS Inc., Canonsburg, USA under the partnership programme (ID-388514).

## IX. REFERENCES

[1]. US patent US20120234445 A1

[2]. Lorna J. Gibson, Michael Ashby, Cellular Solids Structure and Properties, 2nd ed, Cambridge University Press 1999.

[3]. Desmond Moore, Friction in Pneumatic tires, 1st ed, Amsterdam: Elsevier Scientific, 1975.

[4]. Jaehyung Ju, Doo-Man Kim, Kwangwon Kim, "Flexible cellular solid spokes of a non-pneumatic tire," Composite Structures, vol. 94, pp. 2285-2295, January 2012.

[5]. Jaehyung Ju, Doo-Man Kim, Kwangwon Kim, "Static Contact Behaviors of a Non-Pneumatic Tire with Hexagonal Lattice Spokes," SAE International Journal of Passenger Cars-Mechanical Systems, vol. 94, pp. 1518-1527, January 2013

[6]. J. Ju, M. Veeramurthy, J.D. Summers, and L. Thompson, "Rolling Resistance of a Non-Pneumatic Tire having a Porous Elastomer Composite Shear Band", Tire Science and Technology, vol. 41 Issue 3, pp. 154-173, 2013.

[7]. Biao Ma, Yiyong Yang, Yahui Liu," Analysis of vehicle static steering torque based on tire-road contact patch sliding model and variable transmission ratio", Advances in Mechanical Engineering, Vol. 8(9) 1-11, 2016.

[8]. Umesh G C1, Amith Kumar S N, "Design and Analysis of Non-Pneumatic Tyre (NPT) With Honeycomb Spokes Structure", IJESC, vol. 41 Issue 3, pp. 154-173, 2013.

[9]. Moustapha Doumiati, Alessandro Victorino, Ali Charara and Daniel Lechner, "A method to estimate the lateral tire force and the sideslip angle of a vehicle: Experimental validation", American Control Conference,2010

[10]. Sassi S., et.al., "Development of Non-Pneumatic Fiber Composites Tires for Hazard Reduction And Road Safety Improvement", CMVA Annual Seminar on Machinery Vibration

[11]. K.L. Johnson, Contact Mechanics, 1st ed, Cambridge University Press,1985

[12]. Bruce Duncan, The Hyper Elastic Properties of a Polyurethane Adhesive, National Physical Laboratory,2001, ISSN-1361-4061.

[13]. Rafael Tobajas, Elena Ibarz and Luis Gracia, "A comparative study of hyper elastic constitutive models to characterize the behavior of a polymer used in automotive engines",

[14]. Z. Novak, "Constitutive Modelling And Parameter Identification for Rubber-Like Materials", Engng. Trans., Vol 56 No. 2, pp117-157,2008

[15]. Ansys Mechanical APDL Structural Analysis Guide, Ansys Inc.,2017

[16]. Ansys Mechanical APDL Verification Manual, Ansys Inc.,2017

[17]. Ansys Mechanical APDL Theory Reference, Ansys Inc.,2017

[18]. Automobile technical repository: https://www.auto123.com/